land

MDPI

Article

Global Pattern of Vegetation Homogeneity and Its Impact on Land Surface Temperature

Ehsan Rahimi [1], Pinliang Dong [2] and Chuleui Jung [1,3,*]

[1] Agricultural Science and Technology Institute, Andong National University, Andong 36729, Republic of Korea; ehsanrahimi666@gmail.com
[2] Department of Geography and the Environment, University of North Texas, Denton, TX 76205, USA; pinliang.dong@unt.edu
[3] Department of Plant Medical, Andong National University, Andong 36729, Republic of Korea
* Correspondence: cjung@andong.ac.kr

Abstract: Recent advancements in texture-based metrics have improved the representation of landscape heterogeneity, yet global-scale analyses of the relationship between vegetation homogeneity and land surface temperature (LST) remain limited. This study addresses this gap by examining the correlation between Enhanced Vegetation Index (EVI)-derived texture metrics and LST worldwide. We used texture-based metrics from the EVI to assess landscape homogeneity, with LST data from the 2015 MODIS MOD11A1 V6.1 product at a 1 km spatial resolution. Correlation analyses and nonlinear regression models were applied to explore how EVI homogeneity relates to LST across latitudes. Our findings reveal a significant positive correlation between EVI homogeneity and LST, with the strongest association in the Northern Hemisphere (R^2 = 49.3%), followed by a moderate relationship in the Southern Hemisphere (R^2 = 21.1%). In tropical regions (−10° to 10° latitudes), the association is weaker but still significant (R^2 = 15.1%). The distribution of EVI homogeneity follows a Gaussian curve, peaking in mid-latitudes (from −35° to −15° in the Southern Hemisphere and from 15° to 35° in the Northern Hemisphere), while tropical regions exhibit consistently low homogeneity with minimal variation. Our results indicate that regions with higher EVI homogeneity, representing less fragmented vegetation, tend to experience higher LST, whereas areas with more fragmented vegetation (lower homogeneity) exhibit cooler temperatures. Our findings offer valuable insights into the role of vegetation structure in regulating surface temperature across diverse ecosystems. The study highlights the potential for texture-based metrics to enhance environmental monitoring, contributing to improved climate adaptation strategies and sustainable land management practices globally.

Keywords: landscape ecology; enhanced vegetation index; texture metrics; landscape heterogeneity latitudinal variation; MODIS data

check for updates

Academic Editors: Yaqun Liu, Wei Song, Jieyong Wang, Kangwen Zhu, Xuanchang Zhang and Cong Ou

Received: 19 January 2025
Revised: 13 February 2025
Accepted: 15 February 2025
Published: 17 February 2025

Citation: Rahimi, E.; Dong, P.; Jung, C. Global Pattern of Vegetation Homogeneity and Its Impact on Land Surface Temperature. *Land* **2025**, *14*, 421. https://doi.org/10.3390/land14020421

Copyright: © 2025 by the authors. Licensee MDPI, Basel, Switzerland. This article is an open access article distributed under the terms and conditions of the Creative Commons Attribution (CC BY) license (https://creativecommons.org/licenses/by/4.0/).

1. Introduction

Phenomena such as urban expansion exert a considerable impact on LST, primarily due to the dominance of artificial infrastructures in urbanized areas, which leads to elevated temperatures [1,2]. Vegetation, including green spaces, pastures, and forests, plays a crucial role in regulating LST and serves as a key factor in urban heat island (UHI) studies [3–5]. The variations in LST are intricately linked to climate change and are modulated by several elements, including vegetation density, soil composition, construction materials, and

precipitation patterns [6,7]. Consequently, vegetation, in any form, acts as a crucial buffer against global warming by mitigating heat accumulation [8,9].

Recent advancements in landscape ecology have facilitated the analysis of LST through landscape metrics [10] and land use maps, enabling a deeper understanding of the relationship between landscape heterogeneity and temperature variations. Landscape heterogeneity is a fundamental characteristic of ecosystems, influencing biodiversity and ecological functions [11,12]. The spatial configuration and diversity of landscapes are essential for species persistence, habitat connectivity, and ecological community dynamics, thereby playing a vital role in biodiversity conservation and habitat management [12–14]. Understanding how landscape structures relate to ecological processes necessitates the identification of heterogeneity in a manner that corresponds to the studied phenomenon. To achieve this, landscape ecologists frequently employ a discrete framework, conceptualizing landscapes as mosaics composed of distinct patches [15]. One such framework, the patch–corridor–matrix (PCM) model, introduced in the 1980s, characterizes landscape structures as a collection of homogenous patches represented in discrete units, requiring a thematic resolution that ensures effective quantification of heterogeneity [16].

Although the PCM model remains a valuable tool, it does not fully encapsulate the complexities of land surface attributes as its classification relies on aggregated land cover data, which often integrate multiple influencing factors [17,18]. This shortcoming highlights the necessity for more refined methodologies in assessing LST dynamics. Moreover, many commonly used landscape metrics exhibit high correlations, complicating comparisons across different spatial scales [19]. To address these limitations, direct integration of vegetation indices such as the normalized difference vegetation index (NDVI) and the enhanced vegetation index (EVI) has been advocated for studying LST variations within heterogeneous landscapes [20,21]. Continuous methodologies have been proposed as alternatives to conventional discrete models, allowing for a more nuanced representation of landscape heterogeneity [22]. Notably, texture-based metrics, including those derived from the gray level co-occurrence matrix (GLCM), have demonstrated their effectiveness in capturing spatial complexity and thermal variability in urban environments [23–27].

Texture measures offer a way to quantitatively capture how neighboring pixels' digital number (DN) values relate to one another, resulting in a continuous spatial indicator suitable for subsequent analyses. Park et al. [24] investigated the utility of GLCM indices as spatial metrics at the landscape scale. Their study compared eight GLCM parameters with 18 traditional landscape metrics, which addressed aspects such as composition, clustering, dominance, dispersion, and shape complexity. This approach was applied specifically to urban tree canopy studies.

In another investigation, Rahimi et al. [27] contrasted texture-based measures with landscape metrics to evaluate how urban fragmentation influences LST across different spatial extents. Their results revealed that the link between LST and urban heterogeneity intensified as the total area studied increased. Moreover, texture-based measures yielded an average R^2 of about 34.84%, notably higher than the average R^2 of 15.33% for conventional landscape metrics. GLCM-based techniques have also been employed by Iqbal et al. [26] to classify crops at various phenological phases using drone-acquired optical imagery. In that work, grayscale images were used to extract texture features that effectively distinguished different types of crops. Similarly, Rahimi et al. [28] examined vegetation heterogeneity in an urban–agricultural area in Iran by integrating continuous metrics with the NDVI. They reported that texture-driven indicators such as dissimilarity and entropy aligned positively with NDVI variations, indicating increased diversity in plant cover.

Despite the increasing volume of research investigating the relationship between vegetation and LST, a significant gap remains in global-scale studies that employ texture-based

metrics to analyze this interaction across different latitudinal zones. Most prior research has been limited to specific regions and has primarily relied on conventional landscape metrics, which, while useful, may not sufficiently capture the fine-scale spatial heterogeneity of vegetation. Traditional approaches often overlook the intricate spatial patterns and structural complexity of vegetation, which can play a crucial role in regulating surface temperatures. In this context, our study aims to address the following key questions: (1) How does vegetation homogeneity, as quantified through texture-based metrics, correlate with LST at different spatial scales—globally, as well as across northern, southern, and tropical latitudes? (2) To what extent do latitudinal differences influence this relationship, and how do climatic and biogeographical factors modulate the interaction between vegetation structure and surface temperature?

To bridge this knowledge gap, we employ advanced texture-based metrics to systematically assess the correlation between the spatial EVI homogeneity and LST across these latitudinal zones. By leveraging this approach, we aim to elucidate the role of spatial heterogeneity in driving vegetation–LST dynamics on a global scale. This research will not only enhance our understanding of how vegetation structure influences thermal regulation across diverse climatic regions, but will also provide critical insights to improve predictions of surface temperature variations under changing climate conditions and develop targeted mitigation strategies to counteract urban heat islands and ecosystem degradation.

2. Materials and Methods

2.1. Global GLCM Data

We employed texture metrics derived from the EVI imagery obtained from the Moderate Resolution Imaging Spectroradiometer (MODIS) to evaluate landscape heterogeneity. Specifically, EVI homogeneity (Table 1) was analyzed as a primary textural indicator, where higher homogeneity values indicate reduced heterogeneity. Tuanmu et al. [23] introduced a set of 14 heterogeneity metrics, which are accessible via http://www.earthenv.org accessed on 20 December 2024. Among these, they identified a core subset of six metrics that were assessed for their effectiveness in representing fine-scale habitat heterogeneity. Their evaluation included comparisons with 30-m Landsat-based land cover data to determine performance. To assess spatial heterogeneity, EVI-derived metrics were contrasted with more conventional measures, such as topography-based or categorical land cover metrics. Further, spatial autoregressive models were used to investigate the relationship between these heterogeneity metrics and bird species richness across the United States, utilizing data from the Breeding Bird Survey. This dataset allowed us to explore landscape heterogeneity and its potential correlation with LST across different latitudinal regions. Among the 14 heterogeneity metrics, we selected "EVI homogeneity" (Figure 1a) because it exhibited the highest statistical association with LST in a similar study [27] and with vegetation cover in pre-urban agricultural landscapes [28], outperforming other metrics in capturing the relationship between vegetation structure and surface temperature.

Table 1. Homogeneity metric used to assess spatial landscape heterogeneity. This metric quantifies pixel similarity in an image, ranging from 0 (high heterogeneity) to 1 (high homogeneity). The equation defines homogeneity based on pixel co-occurrence probabilities.

Metric	Measure	Value Range	Expected Relationship *	Equation
Homogeneity	A measure of homogenous pixel values across an image	≥0; ≤1	H ∼ −X	$\sum_{i}^{N_g}\sum_{j}^{N_g}\frac{1}{1+(i-j)^2}p_d(i,j)$

* H ∼ −X, lower values indicate greater heterogeneity; N_g: number of gray levels in the image; $p_d(i,j)$: probability of co-occurrence of pixel values i and j.

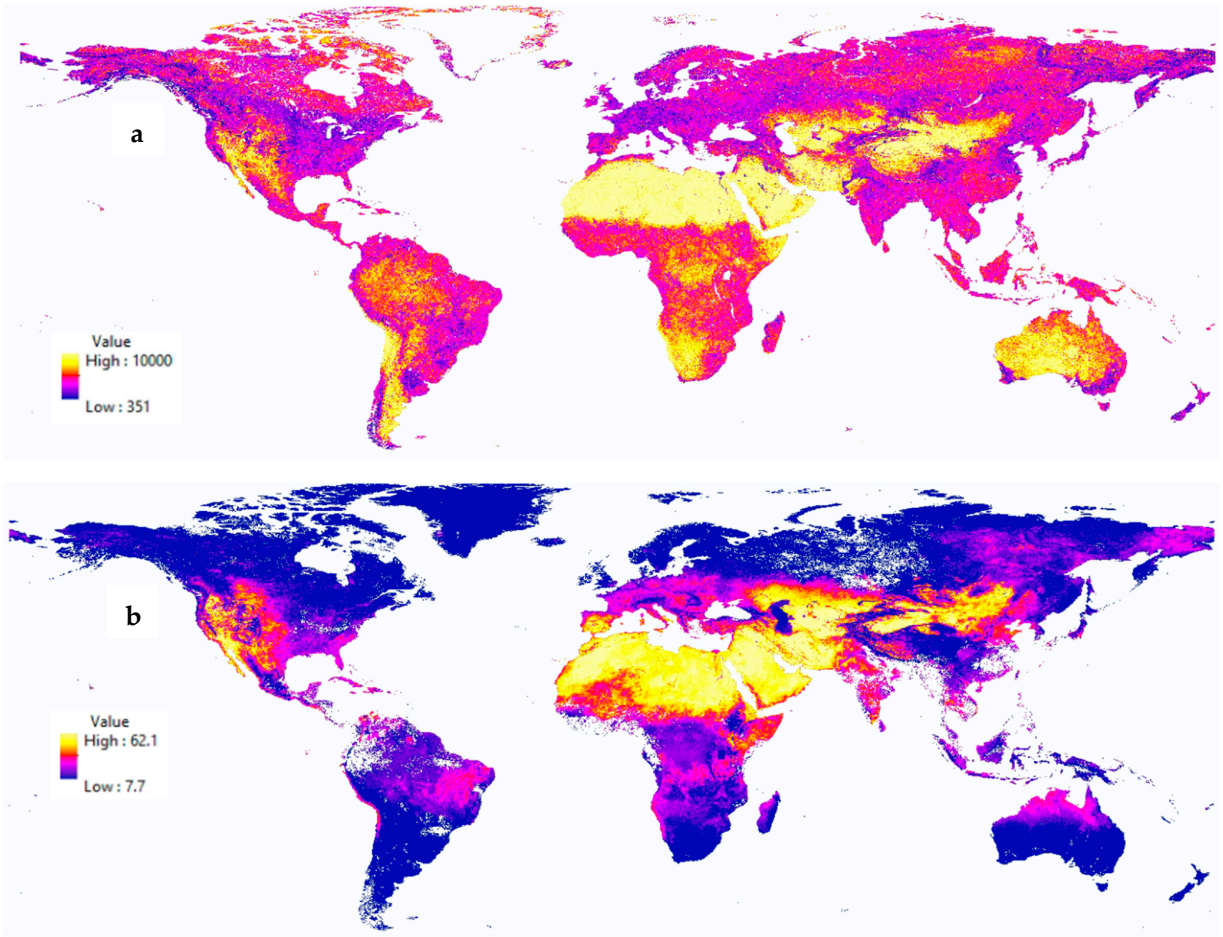


Figure 1. Maps of EVI homogeneity (**a**) and LST (**b**) used in this study. Panel (**a**) displays EVI homogeneity, where yellow areas indicate high values of heterogeneity. Panel (**b**) presents the LST map, with yellow regions corresponding to higher surface temperatures, measured in Celcius.

2.2. Global LST Data

For our study, we obtained LST data for 2015 from the MODIS MOD11A1 V6.1 product, which provides daily global LST and emissivity values at a 1 km spatial resolution (Figure 1b). This dataset, derived from the MOD11_L2 swath product, represents average temperatures under clear-sky conditions. In areas above 30° latitudes, where multiple observations may occur on a single day, the pixel values are averaged across all qualifying clear-sky observations. The MOD11A1 product includes both daytime and nighttime LST bands, as well as quality indicator layers, with thermal infrared observations provided by MODIS bands 31 and 32. To ensure robust data quality, the dataset includes six observation layers. Available through NASA's LP DAAC at the USGS EROS Center, this product is part of a continuous data record from February 2000 to the present (https://lpdaac.usgs.gov/products/mod11a1v061/ accessed on 20 December 2024). The high spatial resolution and daily temporal frequency of this dataset make it an invaluable resource for large-scale environmental studies, including investigations into LST dynamics across diverse ecosystems. For our analysis, we focused on the 2015 LST data to support the specific objectives of our research. Our MODIS data were originally provided in Kelvin units. To make the temperature values more interpretable, we converted them to Celsius using the standard formula: $T(°C) = (LST \times 0.02) - 273.15$. Since the MODIS LST data are scaled by a factor of 0.02, we first multiplied the raw values by this factor to obtain the temperature in Kelvin and then subtracted 273.15 to convert it to Celsius. This ensures that our temperature data align with common climatological conventions and facilitate easier comparison with other temperature datasets.

2.3. Latitudinal Analysis

To investigate the relationship between vegetation heterogeneity and LST across different latitudes, we calculated the average values of both variables for each latitude. We then conducted correlation analyses and applied nonlinear regression models to examine this relationship on a global scale, as well as separately for the Northern and Southern Hemispheres, and within tropical regions (latitudes between -10° and 10°). The analysis was based on two datasets, each containing 16,675 data points spaced at 1 km intervals along the latitudinal gradient. For each data point, we calculated the average EVI homogeneity and extracted the corresponding LST value, along with the latitude. This approach enabled us to systematically explore how EVI homogeneity and LST vary spatially across latitudes. By using nonlinear regression, we aimed to reveal potential nonlinear interactions between these variables, considering the influence of various environmental factors.

Figure 2 presents a flowchart outlining the methodology used in this study. In summary, we assessed landscape heterogeneity by analyzing the homogeneity of EVI imagery based on the dataset provided by Tuanmu et al. [23]. We then acquired LST data from the MODIS MOD11A1 V6.1 product for the same year, with a spatial resolution of 1 km. To investigate the global relationship between vegetation heterogeneity and LST, we performed a latitudinal analysis, computing the average EVI homogeneity and LST values across different latitudes. Using correlation analyses and nonlinear regression models, we examined these relationships on a global scale, as well as separately for the Northern Hemisphere, Southern Hemisphere, and tropical regions, to identify spatial variations and nonlinear interactions influenced by environmental factors.

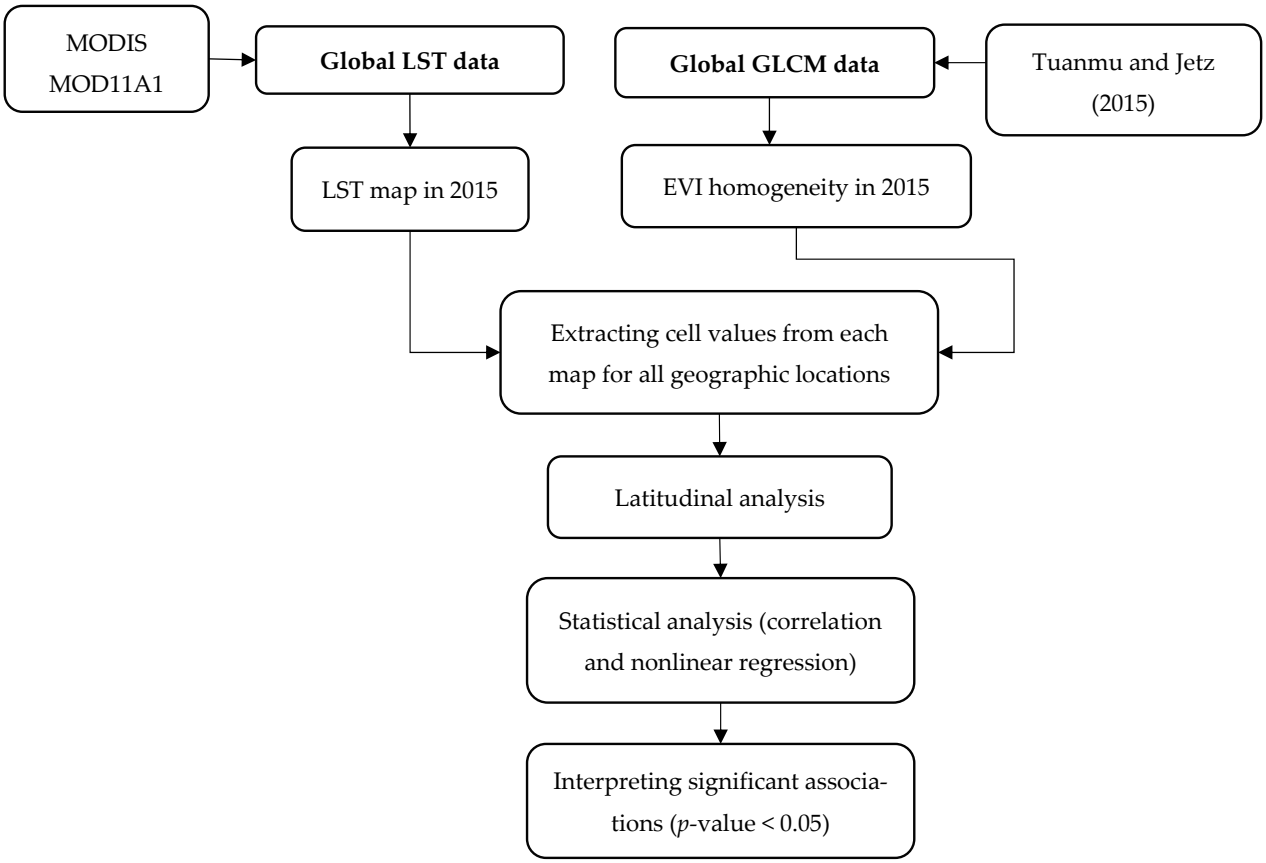


Figure 2. Flowchart of the methodology. This diagram illustrates the study's workflow, including the assessment of landscape heterogeneity using EVI homogeneity, retrieval of LST data from the MODIS, and latitudinal analyses. Correlation and nonlinear regression models were applied to examine the relationship between vegetation heterogeneity and LST globally and across different regions [23].

3. Results

Latitudinal Correlation in EVI Homogeneity and LST

Figure 3 illustrates the average variations in EVI homogeneity across different latitudes. EVI homogeneity follows a Gaussian-shaped distribution, with a peak occurring between −35° and −15° in the Southern Hemisphere, and a similar pattern observed between 15° and 35° in the Northern Hemisphere. In tropical regions, spanning latitudes from −10° to 10°, EVI homogeneity remains relatively low and exhibits minimal variation.

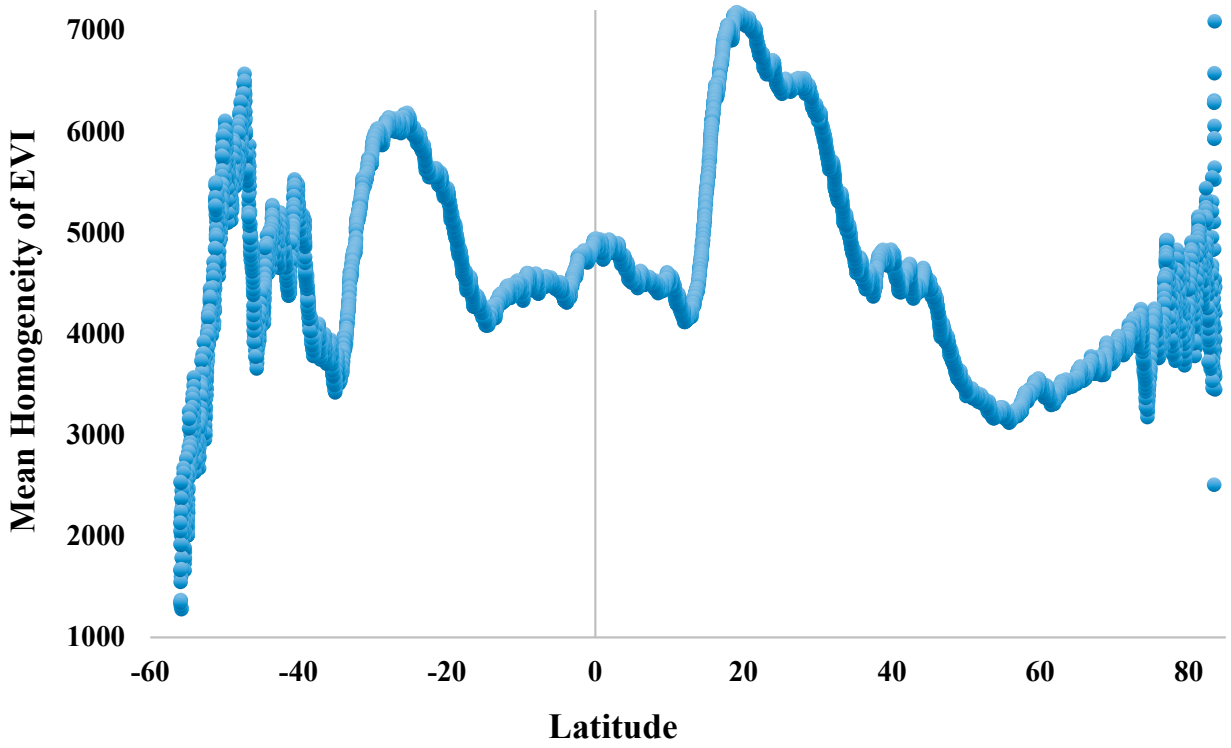


Figure 3. Latitudinal trends in the mean EVI homogeneity. The distribution follows a Gaussian-like pattern, peaking between −35° to −15° in the Southern Hemisphere and between 15° to 35° in the Northern Hemisphere. In tropical regions (−10° to 10° latitudes), EVI homogeneity remains consistently low, with minimal variation.

Table 2 presents the statistical models describing the relationship between EVI homogeneity and LST across different latitude ranges. The quadratic equations and regression metrics provide insights into the strength, direction, and significance of these relationships at global and regional scales. At the global level, EVI homogeneity shows a statistically significant but weak correlation with LST (R^2 = 17.4%). This suggests that while variations in vegetation homogeneity contribute to LST patterns, they only explain a modest portion of the overall LST variability. The positive linear term and small quadratic coefficient indicate a nonlinear but minor influence of homogeneity on temperature. The relationship between EVI homogeneity and LST is strongest in the Northern Hemisphere, with an R^2 value of 49.3%. This indicates that changes in vegetation homogeneity have a more pronounced impact on LST in this region. The higher coefficient for the linear term compared to the global model suggests that increasing homogeneity leads to a stronger warming effect in the Northern Hemisphere.

In the Southern Hemisphere, the correlation remains statistically significant but weaker than in the North (R^2 = 21.1%). While vegetation homogeneity still plays a role in explaining LST variations, other factors likely contribute to temperature dynamics in this region. The negative quadratic coefficient suggests a more complex interaction, where the effect of

homogeneity on LST diminishes at higher homogeneity levels. In tropical regions (−10° to 10° latitudes), the relationship between EVI homogeneity and LST is the weakest among the analyzed regions (R^2 = 15.1%), though still statistically significant. This suggests that while vegetation homogeneity influences temperature, it has a relatively minor effect compared to other environmental factors. The high coefficient for the linear term indicates that at lower latitudes, even small changes in homogeneity could impact LST, but the quadratic term suggests diminishing returns at higher homogeneity levels.

Table 2. Statistical relationship between EVI homogeneity and LST in different latitude ranges. The equations represent quadratic models, with coefficients indicating the strength and direction of the relationship. Statistical metrics include the standard error (S), coefficient of determination (R^2), degrees of freedom (DF), sum of squares (SS), mean square (MS), F-statistic (F), and significance level (*p*-value).

Range	Equation	S	R-sq	DF	SS	MS	F	*p*-Value
Global	LST = 14,104 + 0.08505 EVI homogeneity + 0.000014 EVI homogeneity^2	574	17.4%	2	1,161,742,913	580,871,456	1762.2	0.000
Northern Hemisphere	LST = 13,298 + 0.4907 EVI homogeneity − 0.000021 EVI homogeneity^2	346	49.3%	2	1,166,744,818	583,372,409	4847.9	0.000
Southern Hemisphere	LST = 9445 + 2.081 EVI homogeneity − 0.000210 EVI homogeneity^2	538	21.1%	2	522,017,405	261,008,703	900.6	0.000
−10°–10°	LST = 2190 + 5.470 EVI homogeneity − 0.000579 EVI homogeneity^2	49.8	15.1%	2	1,063,692	531,846	213.6	0.000

Figure 4 highlights the latitudinal trends in the relationship between EVI homogeneity and LST, revealing a predominance of positive correlations. The strongest correlations are observed within the latitude ran ge of 15° to 30°, while closer to the equator (0°), these correlations show a noticeable decline in strength. Upon further analysis, it is evident that 58.7% of the positive correlations occur in the Northern Hemisphere, compared to 41.3% in the Southern Hemisphere. In total, 71.7% of all correlations between EVI homogeneity and LST are positive. This overview includes both statistically significant and non-significant correlations; however, subsequent sections will focus exclusively on significant results for a more in-depth discussion.

Figure 5 displays the *p*-value distribution for correlations between the mean EVI homogeneity and LST across different latitudes. The findings indicate that non-significant correlations are predominantly found in three specific latitude ranges: −80° to −60°, −10° to 0°, and 50° to 80°. Remarkably, 92.1% of the correlations are statistically significant at the 0.05 level, demonstrating a strong overall relationship between these variables. To delve deeper into these significant correlations, a new graph was generated (Figure 6), showcasing their latitudinal trends. While the general patterns align closely with those in Figure 2, an important difference stands out—around 72.3% of the significant correlations are positive, highlighting the prevalence of positive relationships within the dataset.

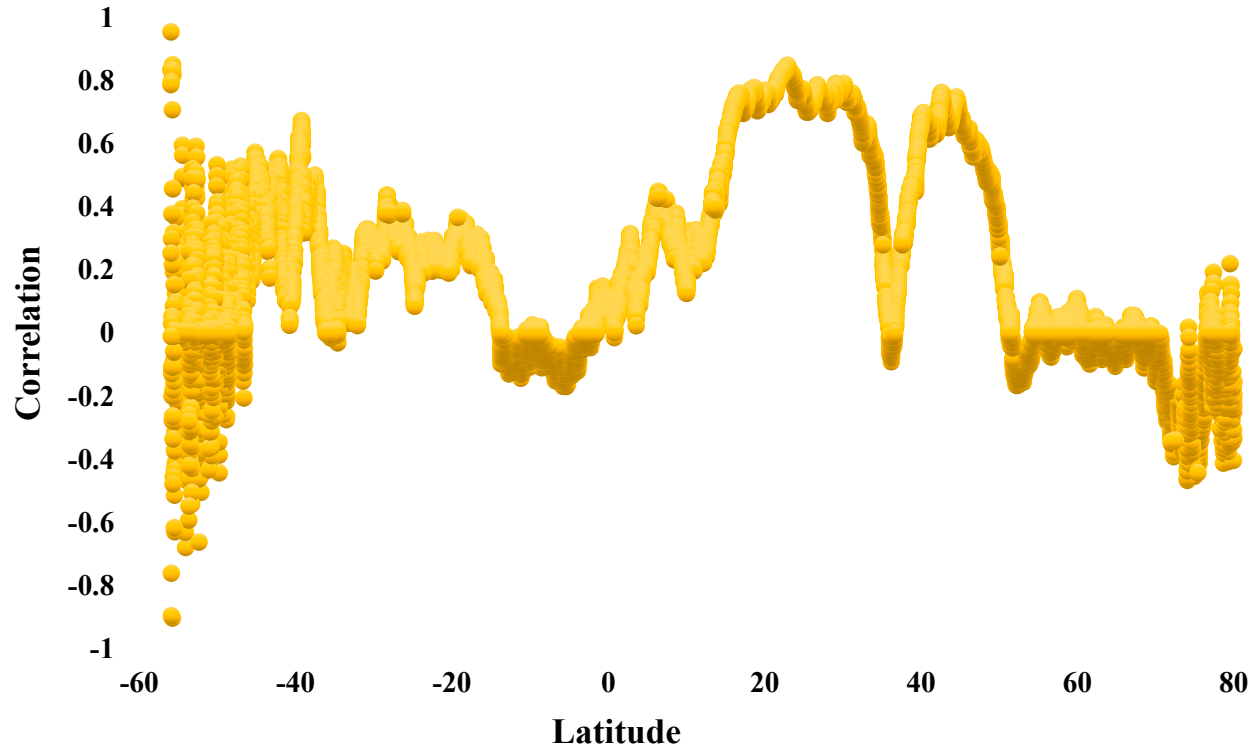


Figure 4. Latitudinal trends in the correlation between EVI homogeneity and LST. Positive correlations dominate, peaking between 15° and 30°, while correlation strength weakens near the equator. A greater proportion of positive correlations is observed in the Northern Hemisphere compared to the Southern Hemisphere. Both significant and non-significant correlations are shown.

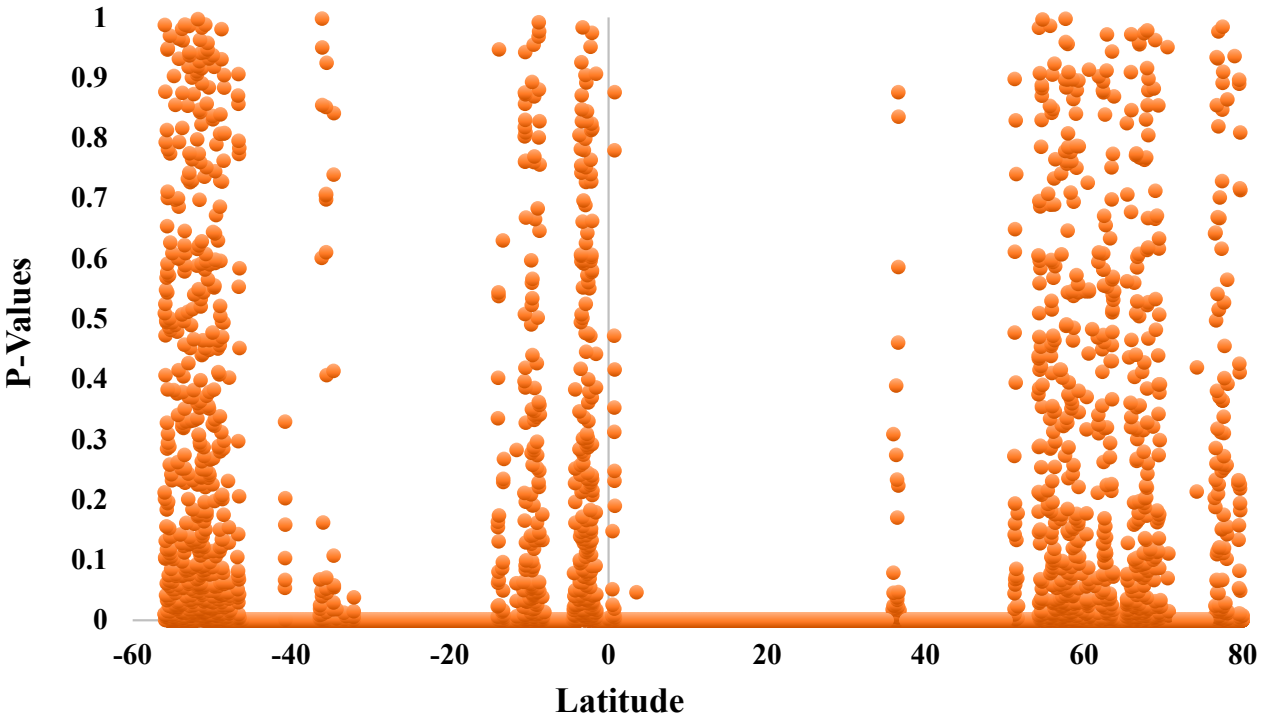


Figure 5. Latitudinal trends in *p*-values of the correlations between EVI homogeneity and LST. Overall, 92.1% of the correlations are statistically significant at the 0.05 level, confirming a strong relationship between these variables.

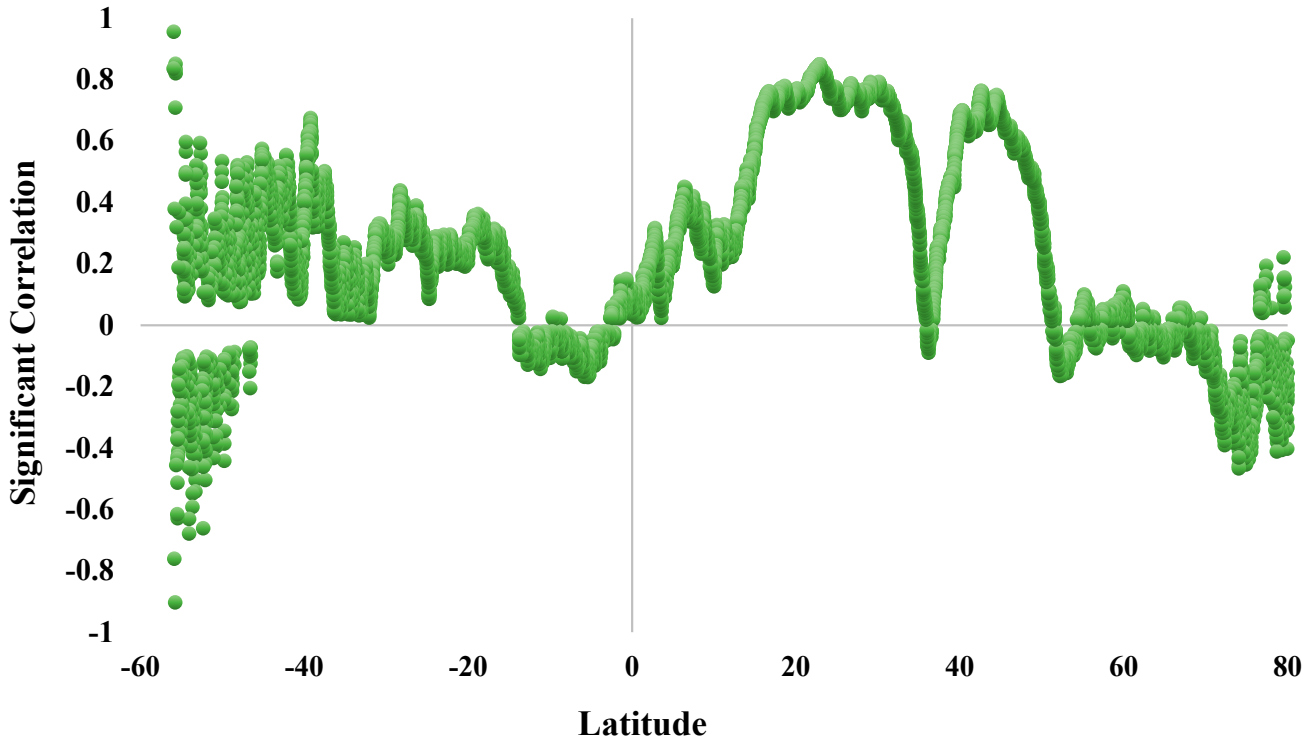


Figure 6. Latitudinal trends in the significant correlations between EVI homogeneity and LST. While the overall pattern resembles Figure 2, a key difference is that 72.3% of the significant correlations are positive, emphasizing the predominance of positive relationships across latitudes.

4. Discussion

The findings of this study provide significant insights into the relationship between EVI homogeneity and LST across latitudes, revealing notable spatial patterns and variability. EVI homogeneity exhibits a Gaussian distribution, peaking in mid-latitudes of both hemispheres (from −35° to −15° in the Southern Hemisphere and from 15° to 35° in the Northern Hemisphere), while tropical regions (−10° to 10°) demonstrate consistently low values with minimal variation. These patterns suggest a strong influence of the latitude on vegetation structure and its spatial uniformity. The statistical analyses underscore the importance of this relationship, albeit with varying strengths across regions.

At a global scale, the association between EVI homogeneity and LST is significant but weak. In contrast, the Northern Hemisphere shows a much stronger relationship (R^2 = 49.3%), indicating a pronounced role of vegetation homogeneity in shaping LST variability in this region. The Southern Hemisphere also exhibits a statistically significant relationship, though the correlation is moderate compared to the Northern Hemisphere. Within tropical regions, the association is weaker but remains significant (R^2 = 15.1%), suggesting that while vegetation homogeneity influences LST, its impact is less pronounced in tropical climates.

Latitudinal trends in correlation strength further reinforce these regional differences. Positive correlations dominate the dataset, particularly in mid-latitudes (15° to 30°), whereas a noticeable decline in correlation strength occurs closer to the equator. Most positive correlations are concentrated in the Northern Hemisphere (58.7%), compared to 41.3% in the Southern Hemisphere, with 71.7% of all correlations being positive. Moreover, a detailed examination of statistical significance reveals that 92.1% of correlations meet the 0.05 significance threshold. These results collectively highlight the latitudinal variation in the relationship between vegetation homogeneity and surface temperature, emphasizing the stronger influence of vegetation structure in mid-latitudes and its relatively diminished

role in tropical regions. By focusing on significant correlations, this study uncovers critical ecological interactions that vary across climatic zones, offering valuable insights into how vegetation patterns mediate land surface processes.

While our models capture significant relationships, the relatively low R^2 values, especially at the global and tropical scales, suggest substantial unexplained variability. Potential outliers—regions where observed LST deviates from model predictions—could be attributed to factors such as land cover differences, where variations in urbanization, water bodies, or barren lands influence LST independently of vegetation homogeneity. Climatic influences, such as cloud cover, humidity, and wind patterns, may also alter LST patterns [29–31] beyond what EVI homogeneity alone can explain. Additionally, the 1 km resolution of the MODIS LST may not fully capture fine-scale temperature variations driven by microclimatic or topographic factors [32,33].

A positive correlation between EVI homogeneity and LST, where lower homogeneity values signify greater vegetation heterogeneity, implies that areas with less fragmented and more uniform vegetation (higher EVI homogeneity) tend to experience elevated LST. In contrast, regions with greater vegetation fragmentation and heterogeneity (lower EVI homogeneity) are associated with reduced LST, suggesting that LST tends to rise when vegetation becomes less fragmented and more uniform. This pattern aligns with findings from a study in Tehran [27], which analyzed the relationship between NDVI homogeneity and LST. The Tehran study reported the regression equation as LST = 35.70 + 0.04 NDVI homogeneity (R^2 = 48.1%, r = 0.69), demonstrating that increased vegetation heterogeneity, indicative of a less uniform vegetation cover, corresponded to a lower LST.

The impact of vegetation patterns on LST has been extensively investigated, with many studies emphasizing the cooling benefits of contiguous vegetation. Research indicates that more aggregated vegetation structures are generally effective in lowering LST due to their ability to provide shade and regulate heat exchange [3,34–39]. However, conflicting results have emerged, suggesting that in certain scenarios, vegetation aggregation may not necessarily contribute to temperature reduction. Studies by Li et al. [3], Maimaitiyiming et al. [40], and Bao et al. [41] found that specific environmental conditions or urban configurations might diminish the cooling efficiency of green spaces.

The influence of landscape composition on LST has been particularly evident in urban environments. Expanding green spaces has been shown to lower temperatures, as demonstrated in studies by Rahimi et al. [27], Guo et al. [42], and Li et al. [35]. In addition, research by Masoudi et al. [43,44] further supports the inverse relationship between LST and landscape metrics associated with green space extent. These studies suggest that larger green patches and cohesive vegetation networks contribute more effectively to temperature mitigation. Guo et al. [42] also noted significant negative correlations between LST and such indicators as the mean patch size (MPS) and the largest patch index (LPI), reinforcing the importance of maintaining extensive, well-connected green areas.

One of the key mechanisms explaining temperature variations in fragmented landscapes is the interplay between patch size and thermal regulation. As vegetation breaks into smaller patches, the overall cooling capacity diminishes due to increased exposure of interior areas to higher ambient temperatures. Smaller patches offer less shading and moisture retention, making them more vulnerable to heat accumulation [45]. In contrast, larger patches maintain cooler temperatures, particularly in their interior regions, where thermal buffering is more effective. The concept of edge effects further explains these patterns, as smaller patches have a higher proportion of edges exposed to direct sunlight and wind, which can lead to increased local temperatures [42].

Furthermore, increased fragmentation leads to higher edge density, which amplifies energy exchange between the patches and their surroundings. This process reduces the

ability of vegetation to mitigate temperature extremes, as more fragmented patches facilitate heat flow from warmer built-up areas, exacerbating LST elevations [46]. These findings highlight the importance of strategic landscape planning that prioritizes larger, contiguous green spaces to counteract the urban heat island effect and promote sustainable temperature regulation. The relationship between vegetation patterns and LST is also dependent on the spatial scale, as demonstrated in multiple studies. Song et al. [47] found that the correlation between green space configurations and LST strengthened as the pixel size increased. Similarly, Lu et al. [48] identified a peak correlation between the NDVI and LST when cell sizes ranged from 210 to 240 m, suggesting that certain spatial resolutions may be optimal for detecting cooling effects. Other research, such as by Xiao et al. [49], observed a progressive increase in the correlation between built-up density and LST as the cell size expanded from 30 m to 960 m.

Conversely, Myint et al. [50] discovered that the influence of impervious surfaces on air temperature began to decline when the analytical window reached approximately 210 m. This indicates that while smaller green spaces may not significantly alter LST, larger spatial scales offer a more comprehensive perspective on temperature mitigation. The findings suggest that future research should further explore the influence of the scale on assessing the LST–vegetation interactions, as varying resolutions may reveal distinct thermal dynamics that inform urban greening strategies. By incorporating multi-scale analyses, researchers can enhance the understanding of how spatial patterns of vegetation interact with urban climates and contribute to more effective environmental planning.

5. Conclusions

This study provides crucial insights into the relationship between vegetation homogeneity and LST across different latitudes, emphasizing the role of spatial vegetation patterns in influencing thermal dynamics on a global scale. The results reveal significant latitudinal variations, with stronger correlations in mid-latitude regions, particularly in the Northern Hemisphere, while the relationship weakens in tropical areas. From a practical perspective, understanding the link between vegetation fragmentation and LST can inform land use planning and conservation efforts. Our findings suggest that maintaining a balance between vegetation continuity and fragmentation is key to regulating temperature variations across diverse ecosystems. For example, in forested regions, minimizing excessive fragmentation could help stabilize local climate conditions by preserving thermal buffering effects.

Based on the study's findings, actionable recommendations include prioritizing policies that support sustainable land management by considering vegetation patterns in climate adaptation efforts. Large-scale afforestation and reforestation programs should account for the spatial arrangement of vegetation to maximize their cooling potential. Conservation planning should integrate knowledge of vegetation–latitude interactions to enhance habitat stability under changing climatic conditions. Additionally, land use policies should avoid excessive homogenization of vegetation in regions where heterogeneity plays a key role in regulating local climate.

Future research should explore the temporal dynamics of vegetation homogeneity and LST interactions for assessing seasonal and long-term trends. Incorporating additional environmental variables, such as soil moisture, albedo, atmospheric circulation, and land cover changes, could improve model accuracy and provide a more comprehensive understanding of the factors driving temperature variability globally. High-resolution remote sensing data (e.g., Landsat and Sentinel data) and multi-scale analyses should be leveraged to refine insights into the vegetation–LST interactions across diverse biomes. Expanding

research across different climatic zones and land cover types would further enhance the applicability of findings for global climate resilience strategies.

Author Contributions: Conceptualization, E.R. and P.D.; Methodology, E.R.; Software, E.R.; Validation, E.R., P.D. and C.J.; Formal analysis, E.R. and C.J.; Investigation, E.R.; Resources, C.J.; Data curation, E.R.; Writing—original draft preparation, E.R.; Writing—review and editing, P.D. and C.J.; Visualization, C.J.; Supervision, P.D. and C.J.; Project administration, C.J.; Funding acquisition, C.J. All authors have read and agreed to the published version of the manuscript.

Funding: This research was funded by RDA Korea, grant No. RS-2023-00232847, and the National Research Foundation of Korea (NRF-2018R1A6A1A03024862).

Data Availability Statement: Data on the correlation details between LST and Homogeneity of NDVI are available at https://github.com/ehsanrahimi666/Global_GLCM.git (accessed on 10 February 2025).

Conflicts of Interest: The authors declare no conflict of interest.

References

1. Roy, S.; Pandit, S.; Eva, E.A.; Bagmar, M.S.H.; Papia, M.; Banik, L.; Dube, T.; Rahman, F.; Razi, M.A. Examining the nexus between land surface temperature and urban growth in Chattogram Metropolitan Area of Bangladesh using long term Landsat series data. *Urban Clim.* **2020**, *32*, 100593. [CrossRef]
2. Rao, Y.; Dai, J.; Dai, D.; He, Q. Effect of urban growth pattern on land surface temperature in China: A multi-scale landscape analysis of 338 cities. *Land Use Policy* **2021**, *103*, 105314. [CrossRef]
3. Li, J.; Song, C.; Cao, L.; Zhu, F.; Meng, X.; Wu, J. Impacts of landscape structure on surface urban heat islands: A case study of Shanghai, China. *Remote Sens. Environ.* **2011**, *115*, 3249–3263. [CrossRef]
4. Gui, X.; Wang, L.; Yao, R.; Yu, D.; Li, C. Investigating the urbanization process and its impact on vegetation change and urban heat island in Wuhan, China. *Environ. Sci. Pollut. Res.* **2019**, *26*, 30808–30825. [CrossRef]
5. Rawat, A.; Singh, H. Role of Urban Forests in Modulating Urban Climate. In *Urban Forests, Climate Change and Environmental Pollution*; Springer: Cham, Switzerland, 2024; pp. 351–371.
6. Adeyeri, O.E.; Folorunsho, A.H.; Ayegbusi, K.I.; Bobde, V.; Adeliyi, T.E.; Ndehedehe, C.E.; Akinsanola, A.A. Land surface dynamics and meteorological forcings modulate land surface temperature characteristics. *Sustain. Cities Soc.* **2024**, *101*, 105072. [CrossRef]
7. Argüeso, D.; Evans, J.P.; Fita, L.; Bormann, K.J. Temperature response to future urbanization and climate change. *Clim. Dyn.* **2014**, *42*, 2183–2199. [CrossRef]
8. Block, A.H.; Livesley, S.; Williams, N.S. *Responding to the Urban Heat Island: A Review of the Potential of Green Infrastructure*; Victorian Centre for Climate Change Adaptation Research: Parkville, Australia, 2012.
9. Espeland, E.K.; Kettenring, K.M. Strategic plant choices can alleviate climate change impacts: A review. *J. Environ. Manag.* **2018**, *222*, 316–324. [CrossRef]
10. Kupfer, J.A. Landscape ecology and biogeography: Rethinking landscape metrics in a post-FRAGSTATS landscape. *Prog. Phys. Geogr.* **2012**, *36*, 400–420. [CrossRef]
11. Sirami, C. Biodiversity in heterogeneous and dynamic landscapes. In *Oxford Research Encyclopedia of Environmental Science*; Oxford University Press: Oxford, UK, 2016.
12. Brose, U.; Hillebrand, H. Biodiversity and ecosystem functioning in dynamic landscapes. *Philos. Trans. R. Soc. B Biol. Sci.* **2016**, *371*, 20150267. [CrossRef]
13. Forman, R.T. Ecologically sustainable landscapes: The role of spatial configuration. In *Changing Landscapes: An Ecological Perspective*; Springer: New York, NY, USA, 1990; pp. 261–278.
14. Tscharntke, T.; Tylianakis, J.M.; Rand, T.A.; Didham, R.K.; Fahrig, L.; Batáry, P.; Bengtsson, J.; Clough, Y.; Crist, T.O.; Dormann, C.F. Landscape moderation of biodiversity patterns and processes-eight hypotheses. *Biol. Rev.* **2012**, *87*, 661–685. [CrossRef]
15. Forman, R.T. *Land Mosaics: The Ecology of Landscapes and Regions*; Cambridge University Press: Cambridge, UK, 1995; Volume 652.
16. Tonetti, V.; Pena, J.C.; Scarpelli, M.D.; Sugai, L.S.; Barros, F.M.; Anunciação, P.R.; Santos, P.M.; Tavares, A.L.; Ribeiro, M.C. Landscape heterogeneity: Concepts, quantification, challenges and future perspectives. *Environ. Conserv.* **2023**, *50*, 83–92. [CrossRef]
17. McGarigal, K.; Tagil, S.; Cushman, S.A. Surface metrics: An alternative to patch metrics for the quantification of landscape structure. *Landsc. Ecol.* **2009**, *24*, 433–450. [CrossRef]
18. Rahimi, E.; Barghjelveh, S.; Dong, P. A comparison of discrete and continuous metrics for measuring landscape changes. *J. Indian Soc. Remote Sens.* **2022**, *50*, 1257–1273. [CrossRef]

19. Kedron, P.J.; Frazier, A.E.; Ovando-Montejo, G.A.; Wang, J. Surface metrics for landscape ecology: A comparison of landscape models across ecoregions and scales. *Landsc. Ecol.* **2018**, *33*, 1489–1504. [CrossRef]
20. De Beurs, K.M.; Henebry, G.M.; Owsley, B.C.; Sokolik, I. Using multiple remote sensing perspectives to identify and attribute land surface dynamics in Central Asia 2001–2013. *Remote Sens. Environ.* **2015**, *170*, 48–61. [CrossRef]
21. Xie, F.; Fan, H. Deriving drought indices from MODIS vegetation indices (NDVI/EVI) and Land Surface Temperature (LST): Is data reconstruction necessary? *Int. J. Appl. Earth Obs. Geoinf.* **2021**, *101*, 102352. [CrossRef]
22. Lausch, A.; Blaschke, T.; Haase, D.; Herzog, F.; Syrbe, R.-U.; Tischendorf, L.; Walz, U. Understanding and quantifying landscape structure—A review on relevant process characteristics, data models and landscape metrics. *Ecol. Model.* **2015**, *295*, 31–41. [CrossRef]
23. Tuanmu, M.N.; Jetz, W. A global, remote sensing-based characterization of terrestrial habitat heterogeneity for biodiversity and ecosystem modelling. *Glob. Ecol. Biogeogr.* **2015**, *24*, 1329–1339. [CrossRef]
24. Park, Y.; Guldmann, J.-M. Measuring continuous landscape patterns with Gray-Level Co-Occurrence Matrix (GLCM) indices: An alternative to patch metrics? *Ecol. Indic.* **2020**, *109*, 105802. [CrossRef]
25. Hall-Beyer, M. Practical guidelines for choosing GLCM textures to use in landscape classification tasks over a range of moderate spatial scales. *Int. J. Remote Sens.* **2017**, *38*, 1312–1338. [CrossRef]
26. Iqbal, N.; Mumtaz, R.; Shafi, U.; Zaidi, S.M.H. Gray level co-occurrence matrix (GLCM) texture based crop classification using low altitude remote sensing platforms. *PeerJ Comput. Sci.* **2021**, *7*, e536. [CrossRef]
27. Rahimi, E.; Barghjelveh, S.; Dong, P. Quantifying how urban landscape heterogeneity affects land surface temperature at multiple scales. *J. Ecol. Environ.* **2021**, *45*, 22. [CrossRef]
28. Rahimi, E.; Jung, C. Analyzing Vegetation Heterogeneity Trends in an Urban-Agricultural Landscape in Iran Using Continuous Metrics and NDVI. *Land* **2025**, *14*, 244. [CrossRef]
29. Deng, X.; Zhao, C.; Yan, H. Systematic modeling of impacts of land use and land cover changes on regional climate: A review. *Adv. Meteorol.* **2013**, *2013*, 317678. [CrossRef]
30. Jiang, Y.; Fu, P.; Weng, Q. Assessing the impacts of urbanization-associated land use/cover change on land surface temperature and surface moisture: A case study in the midwestern United States. *Remote Sens.* **2015**, *7*, 4880–4898. [CrossRef]
31. Qin, Y.; Li, Y.; Xu, R.; Hou, C.; Armstrong, A.; Bach, E.; Wang, Y.; Fu, B. Impacts of 319 wind farms on surface temperature and vegetation in the United States. *Environ. Res. Lett.* **2022**, *17*, 024026. [CrossRef]
32. Wan, Z.; Zhang, Y.; Zhang, Q.; Li, Z.-L. Quality assessment and validation of the MODIS global land surface temperature. *Int. J. Remote Sens.* **2004**, *25*, 261–274. [CrossRef]
33. Yoo, C.; Im, J.; Park, S.; Cho, D. Spatial downscaling of MODIS land surface temperature: Recent research trends, challenges, and future directions. *Korean J. Remote Sens.* **2020**, *36*, 609–626.
34. Estoque, R.C.; Murayama, Y.; Myint, S.W. Effects of landscape composition and pattern on land surface temperature: An urban heat island study in the megacities of Southeast Asia. *Sci. Total Environ.* **2017**, *577*, 349–359. [CrossRef] [PubMed]
35. Li, X.; Zhou, W.; Ouyang, Z.; Xu, W.; Zheng, H. Spatial pattern of greenspace affects land surface temperature: Evidence from the heavily urbanized Beijing metropolitan area, China. *Landsc. Ecol.* **2012**, *27*, 887–898. [CrossRef]
36. Xie, M.; Wang, Y.; Chang, Q.; Fu, M.; Ye, M. Assessment of landscape patterns affecting land surface temperature in different biophysical gradients in Shenzhen, China. *Urban Ecosyst.* **2013**, *16*, 871–886. [CrossRef]
37. Zheng, B.; Myint, S.W.; Fan, C. Spatial configuration of anthropogenic land cover impacts on urban warming. *Landsc. Urban Plan.* **2014**, *130*, 104–111. [CrossRef]
38. Zhang, X.; Zhong, T.; Feng, X.; Wang, K. Estimation of the relationship between vegetation patches and urban land surface temperature with remote sensing. *Int. J. Remote Sens.* **2009**, *30*, 2105–2118. [CrossRef]
39. Zhibin, R.; Haifeng, Z.; Xingyuan, H.; Dan, Z.; Xingyang, Y. Estimation of the relationship between urban vegetation configuration and land surface temperature with remote sensing. *J. Indian Soc. Remote Sens.* **2015**, *43*, 89–100. [CrossRef]
40. Maimaitiyiming, M.; Ghulam, A.; Tiyip, T.; Pla, F.; Latorre-Carmona, P.; Halik, Ü.; Sawut, M.; Caetano, M. Effects of green space spatial pattern on land surface temperature: Implications for sustainable urban planning and climate change adaptation. *ISPRS J. Photogramm. Remote Sens.* **2014**, *89*, 59–66. [CrossRef]
41. Bao, T.; Li, X.; Zhang, J.; Zhang, Y.; Tian, S. Assessing the distribution of urban green spaces and its anisotropic cooling distance on urban heat island pattern in Baotou, China. *ISPRS Int. J. Geo-Inf.* **2016**, *5*, 12. [CrossRef]
42. Guo, G.; Wu, Z.; Chen, Y. Complex mechanisms linking land surface temperature to greenspace spatial patterns: Evidence from four southeastern Chinese cities. *Sci. Total Environ.* **2019**, *674*, 77–87. [CrossRef] [PubMed]
43. Masoudi, M.; Tan, P.Y. Multi-year comparison of the effects of spatial pattern of urban green spaces on urban land surface temperature. *Landsc. Urban Plan.* **2019**, *184*, 44–58. [CrossRef]
44. Masoudi, M.; Tan, P.Y.; Liew, S.C. Multi-city comparison of the relationships between spatial pattern and cooling effect of urban green spaces in four major Asian cities. *Ecol. Indic.* **2019**, *98*, 200–213. [CrossRef]

45. Osborne, P.E.; Alvares-Sanches, T. Quantifying how landscape composition and configuration affect urban land surface temperatures using machine learning and neutral landscapes. *Comput. Environ. Urban Syst.* **2019**, *76*, 80–90. [CrossRef]
46. Wu, C.; Li, J.; Wang, C.; Song, C.; Haase, D.; Breuste, J.; Finka, M. Estimating the cooling effect of pocket green space in high density urban areas in Shanghai, China. *Front. Environ. Sci.* **2021**, *9*, 657969. [CrossRef]
47. Song, J.; Du, S.; Feng, X.; Guo, L. The relationships between landscape compositions and land surface temperature: Quantifying their resolution sensitivity with spatial regression models. *Landsc. Urban Plan.* **2014**, *123*, 145–157. [CrossRef]
48. Lu, L.; Weng, Q.; Xiao, D.; Guo, H.; Li, Q.; Hui, W. Spatiotemporal variation of surface urban heat islands in relation to land cover composition and configuration: A multi-scale case study of Xi'an, China. *Remote Sens.* **2020**, *12*, 2713. [CrossRef]
49. Xiao, R.-b.; Ouyang, Z.-y.; Zheng, H.; Li, W.-f.; Schienke, E.W.; Wang, X.-k. Spatial pattern of impervious surfaces and their impacts on land surface temperature in Beijing, China. *J. Environ. Sci.* **2007**, *19*, 250–256. [CrossRef]
50. Myint, S.W.; Brazel, A.; Okin, G.; Buyantuyev, A. Combined effects of impervious surface and vegetation cover on air temperature variations in a rapidly expanding desert city. *GISci. Remote Sens.* **2010**, *47*, 301–320. [CrossRef]

Disclaimer/Publisher's Note: The statements, opinions and data contained in all publications are solely those of the individual author(s) and contributor(s) and not of MDPI and/or the editor(s). MDPI and/or the editor(s) disclaim responsibility for any injury to people or property resulting from any ideas, methods, instructions or products referred to in the content.